

Reflective three-port grating with a connecting layer under the second Bragg incidence

WENHUA ZHU, BO WANG*, HONGTAO LI, KUNHUA WEN, ZIMING MENG, QU WANG, XIANGJUN XING, LI CHEN, LIANG LEI, JINYUN ZHOU

School of Physics and Optoelectronic Engineering, Guangdong University of Technology, Guangzhou 510006, China

A novel design of reflective three-port polarization-dependent grating with a metal mirror and a connection layer under the second Bragg incidence is reported in this paper. Compared with a description of fused-silica grating at the second Bragg angle, the grating diffraction efficiency for TE polarization is improved. Besides, the wide spectral bandwidth of 109 nm for TM polarization is obtained. Hence, the reflective three-port grating has the advantages of the improvement of diffraction efficiencies for TE polarization and broad spectral bandwidth for TM polarization.

(Received January 16, 2018; accepted November 29, 2018)

Keywords: Three-port splitting, Reflective grating, Polarization dependence, Wide spectral bandwidth

1. Introduction

Power splitters are widely applied in modern optical systems and optical devices, such as photonic integrated circuits [1], polarization control [2], tunable mode-selecting optical filters [3], and writing fiber Bragg device [4]. Rectangular-groove gratings can perform as some beam splitters. Such rectangular-groove beam splitter gratings [5-7] can have merits of high diffraction efficiencies, wide spectral bandwidths and spectral bandwidths [8-10]. Before a beam splitter grating can be designed and fabricated, the grating parameters need to be obtained. Thus, a comprehensive numerical vector method is used to design the numerical parameters, which is known as rigorous coupled-wave analysis (RCWA) method [11, 12]. By using of this rigorous numerical analytical method, Zheng *et al* optimized and designed a three-port grating under second Bragg incidence for TE polarization, where the diffraction efficiencies in the -2nd order, the -1st order and the 0th order are 28.84%, 28.85% and 28.85%, respectively [13]. Although the identical efficiencies have been found, the standard of diffraction efficiencies are necessary to be improved. RCWA merely focuses on doing numerical calculations, which cannot analyze the physical essence about propagation mechanism in grating region. Therefore, a modal method can explain the inherent essence of the coupling modes in the grating [14-16].

In this paper, a three-port grating with a connection layer and a metal slab is designed. Based on using RCWA, high efficiencies in three orders for TE and TM polarizations are obtained with different groove depths and connection layer thicknesses, respectively. Compared with

Ref. [13], such a polarization-dependent device can realize the improved diffraction efficiencies in three orders for TE polarization. Based on utilizing modal method, the reflective diffraction process can be well explained. For investigating the incident bandwidths, the broad spectral bandwidth for TM polarization is obtained. Therefore, the grating is easily produced in new photonics device. The potential fabrication process includes coating, holographic recording and inductively coupled plasma etching.

2. Numerical analysis and modal theory

A principle diagram of three-port grating with a metal mirror and a connection layer under the second Bragg incidence is shown in Fig. 1. Fig. 1 presents a front view of the binary grating, where some parameters are included such as groove depth of h_g^{TE} or h_g^{TM} , depth of connection layer of h_c^{TE} or h_c^{TM} and metal depth of h_m . And a period of grating is set as d . In order to optimize such a grating, the grating material refractive indices of fused silica, Ag and Ta_2O_5 are n_2 , n_m and n_3 , respectively. A TE-polarized wave or TM-polarized wave lights up the grating with a wavelength of λ at the second Bragg angle of θ , where the θ is $\sin^{-1}(\lambda/n_1d)$ and n_1 is the refractive index of air. About the design, some parameters can be given, for instance, h_m is equal to 100 nm, d is 3000 nm, λ is equivalent to 1550 nm. What is more, n_1 , n_2 and n_3 are equal to 1.0, 1.45 and 2.0, respectively. On the basis of the actual etching requirement, the duty cycle of the reflective grating may be chosen to 0.5, which is easily for fabricating and etching.

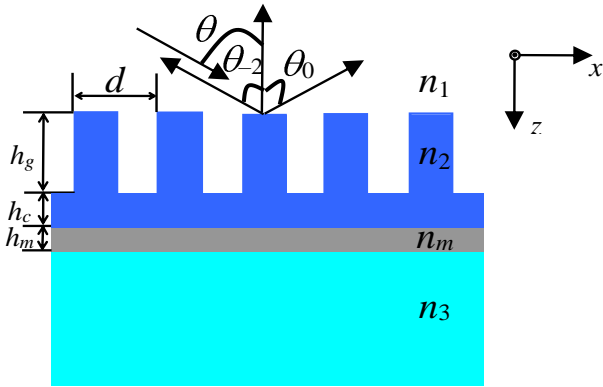


Fig. 1. (Color online) A principle diagram of three-port grating with a metal mirror and a connection layer under the second Bragg incidence

RCWA can use the electromagnetic theory to solve some boundary equations especially for analyzing reflection gratings [17] and obtaining the reflective efficiencies. Therefore, the relevant electromagnetic conditions under the second Bragg incidence are shown in following. In the incident electric field, the incident electric condition is:

$$E_{in,y} = \exp\left[-\frac{2\pi j}{\lambda}\left(\frac{\lambda}{d}x + z\sqrt{1-\frac{\lambda^2}{d^2}}\right)\right] \quad (1)$$

In the incident magnetic field, the incident magnetic equation is that:

$$H_{in,y} = \exp\left[-\frac{2\pi j}{\lambda}\left(\frac{\lambda}{d}x + z\sqrt{1-\frac{\lambda^2}{d^2}}\right)\right] \quad (2)$$

In the reflective electric region, the expression is presented that:

$$E_{R,y} = E_{in,y} + \sum_i R_i \exp\left\{-j\left[\frac{2\pi(1-i)}{d}x - \frac{2\pi\sqrt{d^2-\lambda^2(1-i)^2}}{\lambda d}z\right]\right\} \quad (3)$$

In the reflective magnetic region, the equation is satisfied:

$$H_{R,y} = H_{in,y} + \sum_i R_i \exp\left\{-j\left[\frac{2\pi(1-i)}{d}x - \frac{2\pi\sqrt{d^2-\lambda^2(1-i)^2}}{\lambda d}z\right]\right\} \quad (4)$$

R_i indicates as the amplitude of electric or magnetic field. According to the Maxwell's equation, the whole expression of electric field is gained [11]:

$$H = \left(\frac{j}{\omega\mu}\right)\nabla \times E \quad (5)$$

The equation of magnetic field can be expressed that:

$$E = \left(\frac{-j}{\omega\epsilon n^2}\right)\nabla \times H \quad (6)$$

in which ω , μ , ϵ and n are angular optical frequency, permeability, free space frequency and refractive index about the related area, respectively.

Simultaneous above equations and expanding a series of Fourier equations, the R_i can be obtained. Based on the solved boundary conditions, the reflective efficiencies are shown as:

$$DE_{ri} = R_i R_i^* \operatorname{Re}\left[\frac{\sqrt{d^2-\lambda^2(1-i)^2}}{\lambda\sqrt{d^2-\lambda^2}}\right] \quad (7)$$

Fig. 2 (a) and (b) show diffraction efficiency's ratios of the -1st order to the 0th order and the -2nd order to the -1st order versus the groove depth and the depth of connection layer for TE polarization. In Fig. 2 (a) and (b), under the TE-polarized wave incidence at the second Bragg angle, grating groove depth of h_g^{TE} and connection depth of h_c^{TE} are required to be optimized. A lot of accurate numerical operations can be made by applying the RCWA approach. Based on the calculable numeration, groove depth of $h_g = 1.21 \mu\text{m}$ and depth of connection layer of $h_c = 0.59 \mu\text{m}$ are both obtained. In this situation, the ratio of the -1st order and the 0th order is 1.000, the ratio of the -2nd order to the -1st order is 1.003. For TE polarization, based on the optimized parameters, the efficiencies in the -2nd order, the -1st order and the 0th order are 32.5%, 32.4% and 32.4%, respectively. Fig. 2 (c) shows efficiency's ratio of the -1st order and the 0th order versus groove depth and thickness for TM polarization. Fig. 2 (d) shows efficiency's ratio between the -2nd order and the -1st order versus groove depth and thickness of connection layer for TM polarization. In Fig. 2 (c) and (d), under the TM-polarized wave incidence with a common duty cycle of 0.5 and a wavelength of 1550 nm, the optimal groove depth of h_g^{TM} and depth of connection layer of h_c^{TM} are about $1.09 \mu\text{m}$ and $0.72 \mu\text{m}$, respectively. Based on the optimization of h_g^{TM} and h_c^{TM} , the two splitting ratios of the -1st order to the 0th order and the -2nd order to -1st order are 1.003 and 1.003, respectively. Based on the optimized groove depth and depth of connection layer, TM-polarized light can be reflected the diffraction efficiencies of 32.2%, 32.1% and 32.0% into the -2nd order, the -1st order and the 0th order, respectively.

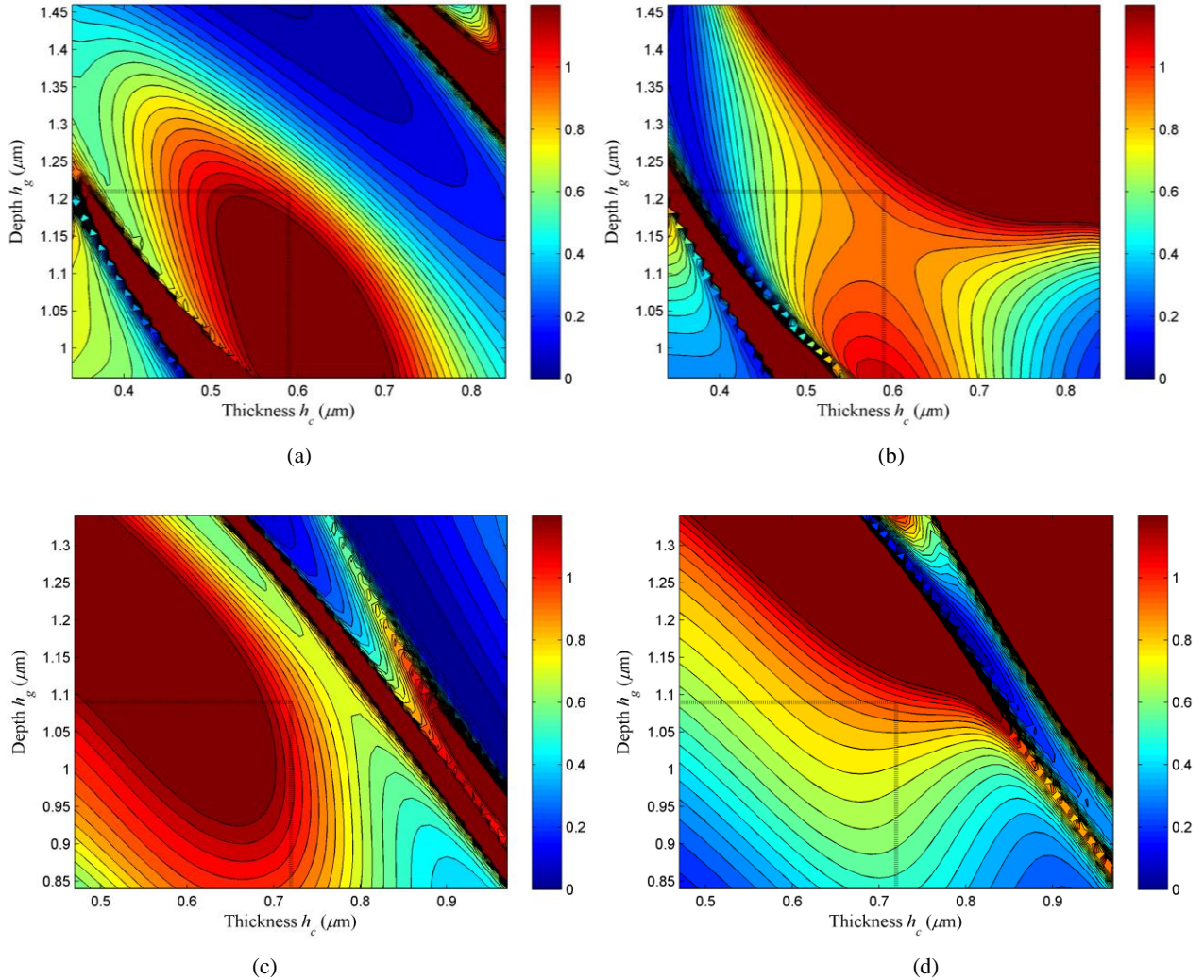


Fig. 2. (Color online) Diffraction efficiency's ratios of the -1st order to the 0th order and the -2nd order to the -1st order versus the grating groove depth and the depth of connection layer: (a) efficiency's ratio of the -1st order and the 0th order for TE polarization, (b) efficiency's ratio of the -2nd order and the -1st order for TE polarization, (c) efficiency's ratio of the -1st order and the 0th order for TM polarization, (d) efficiency's ratio of the -2nd order and the -1st order for TM polarization

Although RCWA method describes a numerical analytical vector method and provides the accurate diffraction efficiencies in three orders for both TE and TM polarizations, the real diffraction process cannot be given for such approach. Hence, a theoretic modal method can state the diffraction process clearly. First, TE- or TM-polarized light can be coupled into some discrete grating modes, where the transition process is called the coupling physical mechanism. In this condition, the ability of coupling efficiency is decided by the overlap integral for TE polarization [16]:

$$\langle E_y^{in}(x) \leftrightarrow u_m(x) \rangle = \frac{\left| \int_0^d E_y^{in}(x) u_m(x) dx \right|^2}{\int_0^d |E_y^{in}(x)|^2 dx \int_0^d |u_m(x)|^2 dx}, \quad (8)$$

for TM polarization, the integral equation is written as:

$$\langle H_y^{in}(x) \leftrightarrow u_p(x) \rangle = \frac{\left| \int_0^d H_y^{in}(x) u_p(x) dx \right|^2}{\int_0^d |H_y^{in}(x)|^2 dx \int_0^d |u_p(x)|^2 dx}. \quad (9)$$

where incident waves are represented by $E_y^{in}(x)$ and $H_y^{in}(x)$, m th grating mode and p th mode are expressed by $u_m(x)$ and $u_p(x)$, respectively. By means of working out the integrals, TE-polarized light takes the 61.30% and 33.10%

energies to mode 0 and mode 2, respectively. Mode 0 and mode 2 can obtain the 54.13% and 33.57% energies, respectively for TM-polarized light. Before the waves can be reflected by the Ag slab, the modes can propagate in the grating with their propagating constants. The propagation constants are determined by effective indices. According to the Eigen functions in Ref. [18], effective indices for both polarizations are $n_{0eff}^{TE} = 1.3964$, $n_{1eff}^{TE} = 1.2300$, $n_{2eff}^{TE} = 1.0059$, $n_{0eff}^{TM} = 1.3802$, $n_{1eff}^{TM} = 1.1750$, $n_{2eff}^{TM} = 1.0034$. When the waves are reflected back to the grating ridge, the waves are diffracted again. Due to the multi-mode interference, the three diffraction orders can be formed for both TE and TM polarizations.

3. Investigation of bandwidths

Although the optimization design of the three-port grating with suitable groove depths of h_g^{TE} and h_g^{TM} and thicknesses of connection layer of h_c^{TE} and h_c^{TM} have been found under a reflective incident wavelength of 1550 nm

and an incident second Bragg angle of 31.11° , some high-efficiency performances are also obtained based on different incident wavelengths and angles under the common duty cycle of 0.5. Fig. 3 shows the reflective efficiency corresponding to the incident wavelength for both of TE and TM polarizations under a usual duty cycle of 0.5. As can be seen from Fig. 3, the incident wavelengths can be varied around the central value of 1550 nm, diffraction efficiencies in the orders are above 30% in a spectral band of 1536-1557 nm for about TE polarization. For the TM polarization, within a broad band range of 1531-1640 nm, the reflective diffraction efficiencies in three orders are over 30%. Fig. 4 shows the diffraction efficiency corresponding to the incident second Bragg angle of θ . In Fig. 4, for investigating the incident angular performance, efficiencies are bigger than 30% in the -2nd order, the -1st order and the 0th order for TE and TM polarizations within the angular band widths range of 29.78° - 32.43° and 29.93° - 32.08° , respectively.

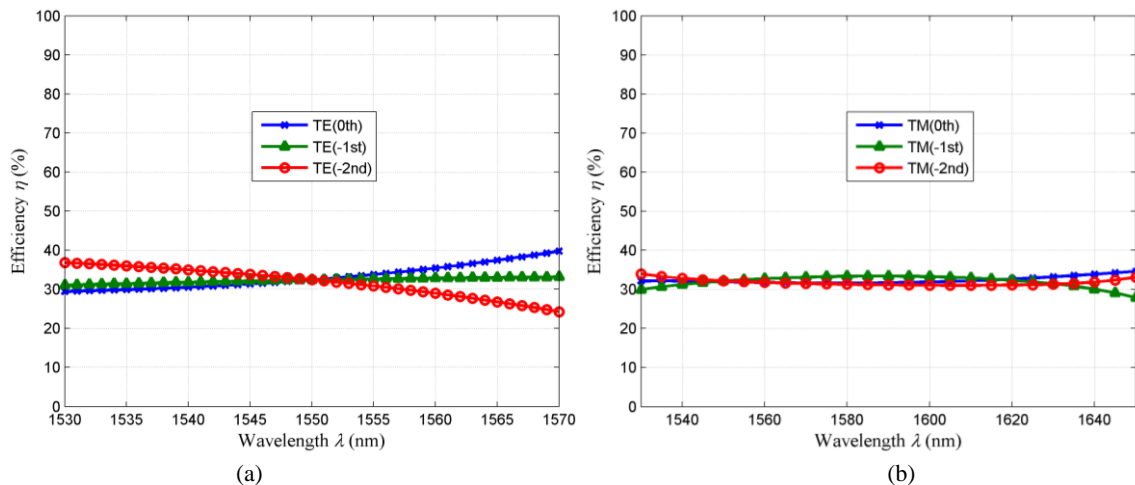


Fig. 3. (Color online) The reflective efficiency corresponding to the incident wavelength for (a) TE polarization and (b) TM polarization under a usual duty cycle of 0.5.

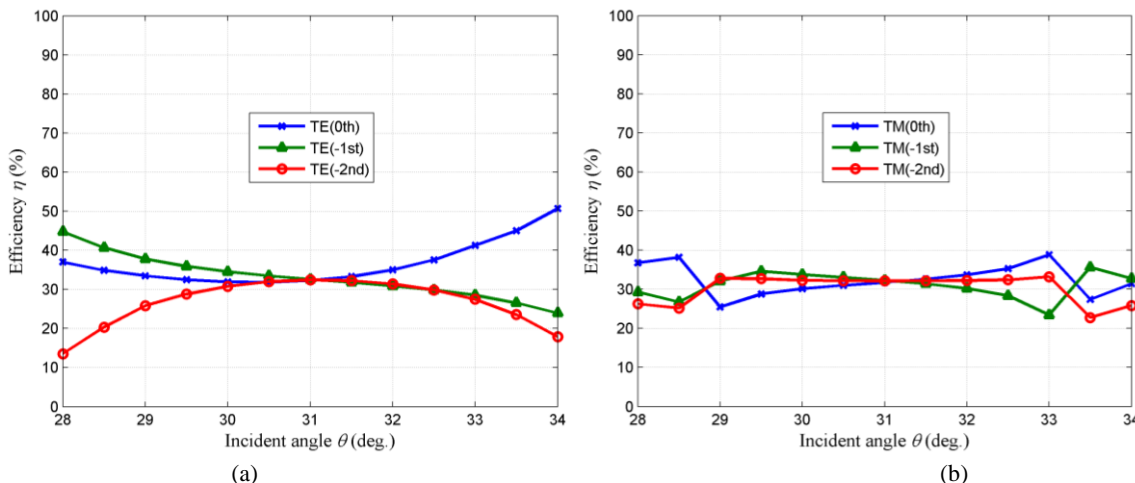


Fig. 4. (Color online) The diffraction efficiency corresponding to the incident second Bragg angle: (a) TE polarization, (b) TM polarization

4. Conclusion

In this paper, we propose and design a reflection connection-layer-based three-port grating under the second Bragg condition by employing rigorous numerical optimization method and theoretical modal analysis method. Based on RCWA method, we have obtained improved diffraction efficiencies in each order for TE polarization and the wide incident spectrum for TM polarization. Due to the metal absorption in reflection three-port grating with a lamellar Ag layer for TE and TM polarizations, the total efficiencies for two polarized waves cannot reach to 100%. Based on modal analysis method, the mechanism of propagation is well interpreted. As a result, the novel grating can help for developing the new photonics device.

Acknowledgements

This work is supported by the Foundation for Distinguished Young Talents in Higher Education of Guangdong (KQNCX065), the Science and Technology Planning Projects of Guangdong Province (2016A020223013, 2016B090918124), and the National Natural Science Foundation of China (11604057, 61475037, 61675050, 11774069).

References

- [1] H. Saghaei, A. Zahedi, R. Karimzadeh, F. Parandin, *Superlattices Microstruct.* **110**, 133 (2017).
- [2] Z. Guo, J. Xiao, *IEEE Photon. Technol. Lett.* **29**(21), 1800 (2017).
- [3] K. Jamshidi-Ghaleh, B. Kazempour, A. Phirouznia, *Superlattices Microstruct.* **101**, 109 (2017).
- [4] B. Wang, *Sci. Rep.* **5**, 16501 (2015).
- [5] W. Fang, X. Fan, X. Zhang, H. Niu, H. Xu, J. Fei, Y. Huang, C. Bai, *IEEE Photon. Technol. Lett.* **30**(8), 708 (2018).
- [6] T. Hu, M. S. Rouifed, H. Qiu, X. Guo, C. G. Littlejohns, C. Liu, H. Wang, *IEEE Photon. Technol. Lett.* **28**(8), 911 (2016).
- [7] J. Xiao, Z. Guo, *IEEE Photon. Technol. Lett.* **30**(6), 529 (2018).
- [8] Q. Bi, J. Zheng, M. Sun, X. Yang, X. Xie, Z. Lin, *Opt. Lett.* **36**(8), 1431 (2011).
- [9] H. Li, B. Wang, H. Pei, L. Chen, L. Lei, J. Zhou, *Superlattices Microstruct.* **93**, 157 (2016).
- [10] H. Guan, H. Chen, J. Wu, Y. Jin, F. Kong, S. Liu, K. Yi, J. Shao, *Opt. Lett.* **39**(1), 170 (2014).
- [11] M. G. Moharam, E. B. Grann, D. A. Pommet, *J. Opt. Soc. Am. A* **12**(5), 1068 (1995).
- [12] M. G. Moharam, D. A. Pommet, E. B. Grann, T. K. Gaylord, *J. Opt. Soc. Am. A* **12**(5), 1077 (1995).
- [13] J. Zheng, C. Zhou, B. Wang, J. Feng, *J. Opt. Soc. Am. A* **25**(5), 1075 (2008).
- [14] I. C. Botten, M. S. Craig, R. C. McPhedran, J. L. Adams, J. R. Andrewartha, *Opt. Acta* **28**(3), 413 (1981).
- [15] H. Wei, L. Li, *Appl. Opt.* **42**(31), 6255 (2003).
- [16] A. Yariv, *IEEE J. Quantum Electron.* **9**(9), 919 (1973).
- [17] M. G. Moharam, T. K. Gaylord, *Appl. Opt.* **20**(2), 240 (1981).
- [18] A. Hu, C. Zhou, H. Cao, J. Wu, J. Yu, W. Jia, *Appl. Opt.* **51**(20), 4902 (2012).

*Corresponding author: wangb_wsx@yeah.net